Energy & Environmental Science

COMMUNICATION

View Article Online
View Journal | View Issue

CrossMark click for updates

Cite this: *Energy Environ. Sci.*, 2014, 7, 3313

Received 17th July 2014
Accepted 5th August 2014

DOI: 10.1039/c4ee02236j

www.rsc.org/ees

Published on 26 August 2014. Downloaded by Northeastern University on 30/12/2015 02:25:48.

Highly transparent paper with tunable haze for green electronics

Zhiqiang Fang,† Hongli Zhu,† Wenzhong Bao,† Colin Preston, Zhen Liu, Jiaqi Dai, Yuanyuan Li and Liangbing Hu*

The ability to manage the light scattering effect of transparent paper without sacrificing its original high transmittance is critical for the application in optoelectronics since different devices have different requirements for the optical properties. In this paper, we study highly transparent paper with a tunable transmission haze by rationally managing the ratio of nanoscale cellulose fibers to macroscopic cellulose fibers. The transparent papers present a largely modulated light scattering behavior while retaining a transparency of over 90%. Various measurements are then used to characterize the optical properties of the different transparent papers in detail. To demonstrate the device applications in green electronics, we fabricated a top gated transistor with MoS_2 on the transparent paper containing 100% NFC that leads to an excellent on/off ratio. The highly transparent paper with a controllable light scattering behavior has an unprecedented potential for applications in optoelectronic devices as a substrate or a functional component.

Broader context

Transparent paper made of cellulose has attracted increased interest in the scientific community because it enables lighter, cheaper, more flexible, and environmentally benign electronics of the future. The ability to modulate the dimension of cellulose fibers in the nanoscale and microsized range by advanced processes enables paper to possess a tailored light scattering effect while maintaining high optical transmittance. Tunable optical haze is a performance-enhancing characteristic of transparent paper compared to plastics used in flexible electronics, because paper is not only a substrate but also a functional component for electronics. This characteristic has great potential to open up new opportunities for transparent paper. As a proof-of-concept, we demonstrated a high-performance MoS_2 transistor on a highly transparent paper.

Introduction

Paper made of cellulose nanofibers is emerging as a substrate in electronic devices due to its earth abundance, remarkable optical and mechanical properties, superior thermal stability, prominent surface smoothness, nontoxicity, excellent printability, and biodegradability.[1–9] Optical properties, such as transparency and transmission haze, are very significant in the fabrication of optoelectronic devices with a tailored performance[10–13] and a light diffusion film, which is widely used in LED light systems, backlight units (BLUs) of liquid crystal displays (LCDs), and signage.[14–16] For paper made of pure cellulose fibers using a similar fabrication method, optical properties primarily depend on the fiber diameter. Cellulose fibers obtained from wood and plants are elongated and hollow cells, with an average diameter of 20–50 μm and a length of 1–3 mm. They have a hierarchical structure comprised of millions of elementary fibrils with a diameter of 3.5–5 nm.[17–19] The elementary fibrils are bundled into microfibrils (5–50 nm in diameter and several microns in length) that further aggregate into microfibril bundles. The hierarchical structure of cellulose fibers enables the production of fibers with diameters ranging from microscale to nanoscale by chemical and/or mechanical treatments. Controlled fiber dimensions directly influence the fabrication of paper with tailored optical properties.[20,21]

In this work, we proposed a facile method to manage the optical properties of paper through a rational design. TEMPO (2,2,6,6-tetramethylpiperidine-1-oxyl radical)-oxidized microsized wood fibers with an average diameter of ~27 μm and an average length of 0.92 mm were used to enhance the haze of the paper, while NFC (nanofibrillated cellulose) with a diameter of ~30 nm was used to decrease the haze of the paper. By adjusting the weight ratio of the TEMPO-oxidized wood fibers to the NFC, the transparent paper fabricated by vacuum filtration possesses a tunable haze from 18% to 60% while retaining a transmittance of over 90%. In addition, a scattering angular distribution measurement was conducted to elucidate the light scattering effect of various transparent papers with a different haze and a high-performance transistor with a MoS_2 nanoflake as a semiconductor was demonstrated.

Department of Materials Science and Engineering, University of Maryland College Park, College Park, Maryland, 20742, USA. E-mail: binghu@umd.edu

† Equally contributed.

Published on 26 August 2014. Downloaded by Northeastern University on 30/12/2015 02:25:48.

Experimental

Preparation of TEMPO-oxidized wood fibers and NFC

Bleached pulp obtained from southern yellow pine trees was disintegrated into a 1 wt% fiber suspension with distilled water and then treated in a TEMPO/NaClO/NaBr system at pH 10.5.[22,23] The suspension was continuously stirred with a Turrax mixer until the color of the water changed from yellow to colorless. The obtained TEMPO-oxidized pulp was then rinsed with distilled water three times to remove the residue chemicals. A portion of the clean TEMPO-oxidized wood pulp was once homogenized in a Microfluidizer processor with a channel diameter of 200 μm under a pressure of 20 000 psi to produce NFC.

Fabrication of transparent paper substrates with a different transmission haze

The transmission haze of the transparent paper substrates was tuned by regulating the weight ratio of the TEMPO-oxidized wood fibers to the NFC. The mixture (1%) of the NFC and the TEMPO-oxidized wood pulp was stirred with a Turrax mixer (IKA, RW20 digital) at a speed of 700 rpm for 30 min and then filtrated with a Buchner funnel using a 90 mm filter membrane (0.65 μm DVPP, Millipore, U.S.A). The time of filtration ranges from 40 min to 6 h depending on the weight ratio of the NFC. The prepared wet paper was sandwiched between two stacks of regular filter paper, placed in a presser under a pressure of 4 MPa and dried at room temperature.

Results and discussion

TEMPO-oxidized wood fibers and NFC were utilized to prepare transparent paper with a tailored optical haze. As shown in Fig. 1a, wood fibers extracted from trees by mature pulping technologies were oxidized using an aqueous TEMPO oxidation system (TEMPO/NaClO/NaBr) at pH 10.5 to prepare the TEMPO-treated wood fibers; NFC was prepared by a homogenization process. When an electromagnetic (EM) wave encounters a TEMPO-oxidized wood fiber, the incident light is strongly scattered due to the micro-sized diameter of the fiber (see the top right part of the schematic of Fig. 1a). As the wood fibers are homogenized into NFC with a diameter of 5–30 nm, the light scatter behavior is sufficiently suppressed because the diameter of NFC is much smaller than the wavelength of visible light, ranging from 400 to 800 nm (see the bottom right part of the schematic of Fig. 1a).

The fiber morphology plays an important role in the fabrication of transparent paper. Here, optical microscopy was used to observe the morphology of the TEMPO-oxidized wood pulp, and the morphology of the NFC was obtained by AFM. Due to the hollow structure and the micro-sized diameter of the wood fibers, it is difficult to produce highly optical transparent paper without mechanical and chemical treatments. To make the wood fibers more suitable for producing transparent paper, a TEMPO oxidation system was used to modify the morphology of the wood fibers by introducing carboxyl groups to the cellulose. As shown in Fig. 1b and c, the wood fibers were cleaved and partially unzipped in the axial direction during the TEMPO treatment and the inset in Fig. 1b presents the uniform and translucent wood fiber suspension (1 wt%) after TEMPO processing. Fig. 1d and e show the fiber length and width distribution of the TEMPO-oxidized wood fibers, respectively. Most TEMPO-oxidized wood fibers are 0.5–2 mm long and 16–32 μm wide. An image of the NFC suspension (1.0 wt%) obtained from homogenization is shown in Fig. 1f and Fig. 1g shows an AFM image of the NFC, illustrating that most of the NFC has a length of less than 1 μm and a width of approximately 30 nm.

Transparent paper was simply fabricated by a vacuum filtration and then dried at atmospheric temperature under pressure. By regulating the weight ratio of the TEMPO-oxidized pulp to NFC, transparent paper with tunable optical properties was obtained. Fig. 2 demonstrates the visual appearance of the transparent papers containing different contents of NFC. The transparent papers were in close contact with the pattern underneath in order to minimize the light scattering of the papers on the visual transparency observed by the human eye. In Fig. 2a–e, the pattern behind the various transparent papers can be clearly observed regardless of the varying NFC contents in the papers, revealing that the designed method to regulate the transmission haze of the papers does not influence the optical transmittance. The regular paper, shown in Fig. 2f, exhibits a high opacity due to extensive light scattering at the fiber surfaces.

To further verify that the transmission haze of our transparent paper may be tuned while retaining highly optical transparency, a UV-Vis spectrometer with an integrating sphere (PerkinElmer® USA) was used to measure the total transmittance and transmission haze of the transparent paper in a wavelength range of 400 nm to 1100 nm. The principle for haze and total optical transmittance testing is explained extensively in previous literature.[20,24,25] Total optical transmittance spectra of each transparent paper with a different content of NFC are shown in Fig. 3a, revealing that the transparent paper fabricated by this method exhibits over 90% transparency. In addition to excellent optical transparency, the transparent paper substrates display a variable transmission haze from 18% to 60% in the visible wavelength range as well (Fig. 3b). Due to an extensive light diffusing behavior of the micro-sized TEMO-oxidized fibers, the transparent paper without the NFC presents the highest transmission haze (~60%), and with an increase in the NFC content in the paper the transmission haze demonstrates a decreasing trend. According to this data and analysis, it is possible to regulate the light scattering effect of the transparent paper by rationally adjusting the weight ratio of the TEMPO-oxidized wood fibers to NFC, while maintaining the transparency over 90% at a wavelength of 550 nm. These tunable optical properties illustrate the potential application of transparent paper in light diffusion films and optoelectronic devices, such as outdoor displays and solar cells.

In order to visualize the light scattering behavior of the transparent paper with different NFC contents, it is shown that a green laser beam with a wavelength of 540 nm travels through the transparent paper and illuminates an area on the target with

 This journal is © The Royal Society of Chemistry 2014

Published on 26 August 2014. Downloaded by Northeastern University on 30/12/2015 02:25:48.

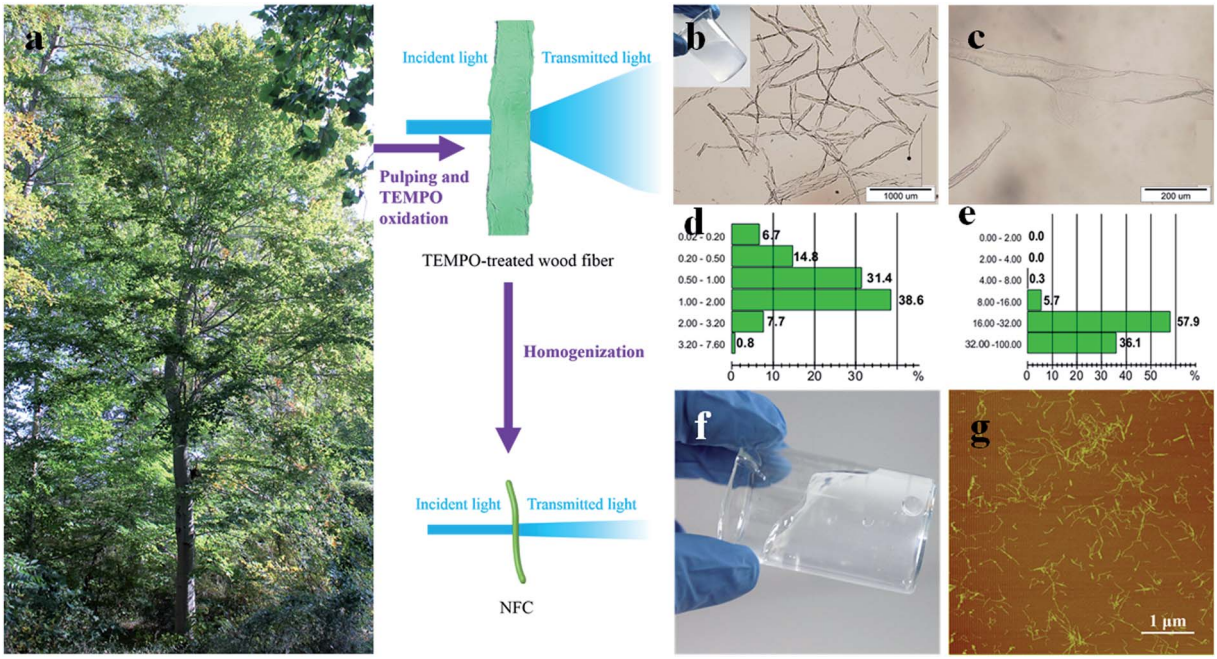

Fig. 1 (a) Flowchart showing the procedure of preparing NFC from trees (the schematic shows the light scattering effect of a TEMPO-oxidized wood fiber (top right) and NFC (bottom right)); optical microscopy images of (b) TEMPO-oxidized wood fibers (the inset shows the TEMPO-oxidized wood fiber suspension) and (c) an unzipped TEMPO-oxidized wood fiber; (d) length fraction of the TEMPO-oxidized wood fibers, the *y*-axis unit is in mm; (e) width fraction of the TEMPO-oxidized wood fibers, the *y*-axis unit is in µm; (f) digital photo of the 1 wt% NFC suspension; (g) AFM image of NFC.

a certain radius. As shown in Fig. 3c, the transmitted light passing through poly(ethylene terephthalate) (PET) shows the smallest luminous radius on the target. This visualizes the low transmission haze of PET <1%, and further indicates that the light scattering caused by PET is negligible. Transparent paper containing a dissimilar NFC content illuminates a larger area on the target compared to PET. As the NFC content within the transparent paper decreases, a larger and more homogeneous illuminated area is gradually observed. Light passing through the transparent paper with 100% NFC shows a small and intense illuminated area on the target (Fig. 3d), due to the fact that most of the incident light transmits straight through the paper. The light scattering effect of the transparent paper with 50% NFC is visualized in Fig. 3e. It is clearly visible that the transmitted light is strongly scattered, resulting in a larger illuminated area. However, the light intensity at the center of the target is more intense than at the edge. A more uniform and larger illuminated area is achieved when the incident light propagates through the transparent paper without NFC (Fig. 3f). Scientists have found that a larger fiber diameter leads to a

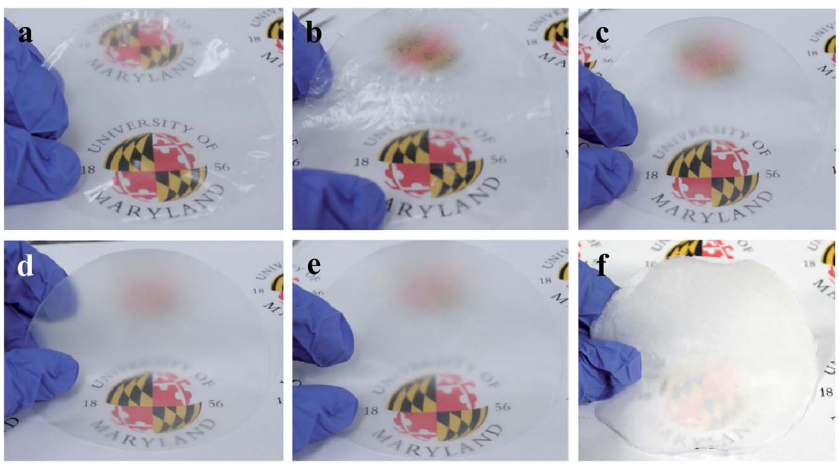

Fig. 2 Optical photos of highly transparent papers with tunable optical properties made of TEMPO-oxidized micro-sized wood fibers and/or NFC, with an NFC content of (a) 100%, (b) 80%, (c) 50%, (d) 20%, and (e) 0%, and of (f) a regular paper.

Published on 26 August 2014. Downloaded by Northeastern University on 30/12/2015 02:25:48.

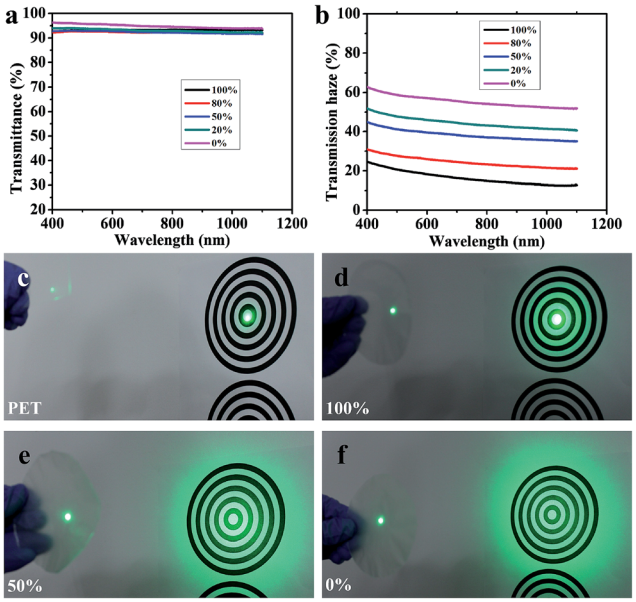

Fig. 3 (a) Light transmittance and (b) transmission haze of the transparent papers with a different content of NFC in the entire paper (100%, 80%, 50%, 20%, and 0%); light scattering effect of the substrates: (c) PET; (d) transparent paper made of pure NFC; (e) transparent paper containing 50% NFC; (f) transparent paper without NFC. Note that the diameter of the laser point is 0.4 mm and the distance between the paper and the target is 30 cm. The maximum diameter of the concentric circles on the target is 14.5 cm.

higher transmission haze.[20,24] The diameter of the fibers and the packing density of the transparent paper play a significant role in its light scattering behavior. In this study, the transparent paper has a thickness of 45–51 μm and a packing density of approximately 1.1–1.2 g cm^{-3}, thus the content of the micro-sized fibers within the transparent paper plays a crucial role in light scattering.

The transmission haze may be defined as the percent of the transmitted beam of light that deviates from the incident beam by more than 2.5° due to light scattering within the bulk of the film.[26] During the fabrication of optoelectronic devices on transparent substrates, the percent of incident light that passes through a transparent substrate must be as high as possible; moreover, transmission haze is also a crucial parameter that should be taken into consideration. A higher haze renders diffuse scattered light, which is beneficial in devices such as solar cells, where stronger light scattering enhances the path of light and induces improved light trapping within the active layer of solar cells.[24,25,27] A high haze also contributes to the uniform light distribution behavior of light diffuser films for LED lighting or backlight units in an LCD.[14,16] Moderate light scattering provides anti-glaring, which ensures comfortable visibility for outdoor devices such as touch panels.[28] A high clarity is desirable in displays in order to achieve vivid and clear images.

To intuitively show how the transmission haze in the paper effects the visibility through the substrate, all samples were placed in a bright environment and the visual appearances of the transparent paper with a different transmission haze are displayed in Fig. 4a–c. The corresponding weight ratio of NFC to total fibers is 100%, 50%, and 0%, respectively. With a decrease in NFC content in the transparent paper, the scene behind the transparent paper gradually becomes obscure. The reason for this phenomenon is the high content of micro-sized fibers within the paper, which causes intensive light scattering that reduces the light intensity per area and makes the image behind the transparent paper more and more turbid.

The transmission haze can be quantified by UV-Vis spectrometry measurements with an integrating sphere, but the accurate behavior of the scattered light is still unknown. An additional experiment was conducted to measure the angular distribution of the scattered light to further elucidate the optical haze of the transparent paper based on our previous work.[25] A paper sample was placed between a rotating detector and a 540 nm laser light source. To measure the scattering angle distribution, the detector rotated behind the sample surfaces from 60° to 120° to collect the intensity of the transmitted light. The scattering angle distribution of the transmitted light for the various transparent paper substrates is displayed in Fig. 4d, which coincides with the transmission haze described in the previous section. For the transparent papers consisting of 100% and 80% NFC, the angular distribution of the transmitted light mainly concentrates in the incident direction. As the NFC content decreases, the peak of the scattering angle distribution curve reduces dramatically, which indicates that the transparent paper with a lower NFC content may cause more intense light scattering that uniformly distributes transmitted light in all directions. In addition to the scattering angle distribution curve of the dissimilar transparent papers, a maximum scattering angle is also used to describe the light scattering extent in this paper. We define the scattering angle range as the scattered light, which illustrates a light intensity larger than 5% of the peak intensity at 90°. The maximum scattering angle of diffusely transmitted light through the transparent paper without NFC is 36° (Fig. 4e), which decreases to 32°, 24°, 14°, and 12° as the NFC content decreases in the transparent papers (as can be seen in Fig. 4f–i).

Scanning electron microscopy (SEM) was used to explore why the transparent papers, which include varying NFC contents, exhibit high optical transmittance. Fig. 5 shows top-view SEM images illustrating the surface morphologies of the transparent papers with different weight ratios of NFC to total fibers and the regular paper made of original fibers without chemical treatments or mechanical processes. Fig. 5a shows the surface morphology of the transparent paper made of pure NFC. There are no obvious cavities observed on the surface, as previously reported. NFC with a diameter of 5–30 nm formed a dense fiber network that reduces light scattering caused by the mismatch refractive index between air (1.0) and the surface of the cellulose fibers (1.5).[29] As shown in Fig. 5b–e, more micro-sized fibers are observed on the surface of the paper as the NFC content in the paper decreases, but the pores in the bulk paper are still significantly suppressed due to the extensive collapse of the fiber cell walls after the TEMPO treatment and the infiltration of NFC in the void spaces of the paper. The TEMPO-treated fibers

 This journal is © The Royal Society of Chemistry 2014

Published on 26 August 2014. Downloaded by Northeastern University on 30/12/2015 02:25:48.

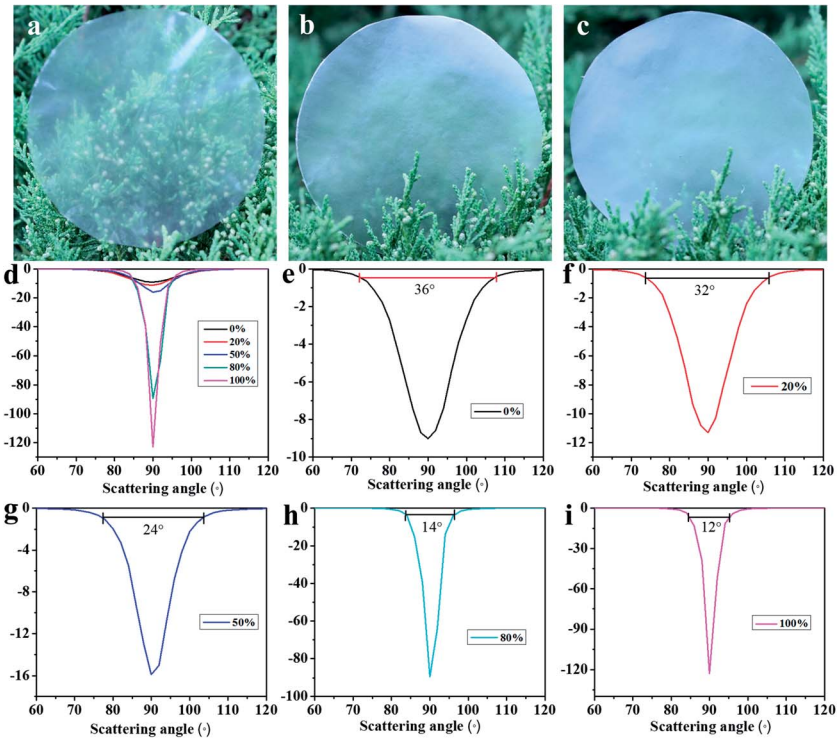

Fig. 4 Visual appearances of the transparent papers with NFC contents of 100% (a), 50% (b), and 0% (c), respectively. (d) Scattering angular distribution with arbitrary *y*-axis units for the various transparent papers. Maximum scattering angle for the transparent papers with a different ratio of NFC to the whole paper: (e) 0%, (f) 20%, (g) 50%, (h) 80%, and (i) 100% NFC.

are prone to being crushed during the filtration and drying process, which results in a higher packing density for the dried paper. Fig. 5e shows a top-view SEM image of the transparent paper consisting of the TEMPO-oxidized micro-sized wood fibers. In comparison to the regular paper shown in Fig. 5f, it shows a higher packing density and better optical transmittance due to the decreased fiber length, increased fiber content and easy collapse of the hollow structured fibers after the TEMPO treatment. The porous structure is apparent in the SEM image of the regular paper, which causes strong light scattering that results in the opacity of the regular paper.

In addition, color difference is another parameter that should be taken into account during the fabrication of transparent paper with different light scattering behavior. Currently, the most complete color space to describe the visible colors for the human eye is CIELAB specified by CIE (International Commission on Illumination): L^* represents the lightness of the color, a low number (0–50) indicates dark and a high number (51–100) refers to light. a^* indicates the difference between green ($-a$) and red ($+a$), b^* refers to the difference between yellow ($+b$) and blue ($-b$). In this study, Technidyne Color Touch PC was used to measure L^*, a^*; and b^* of the

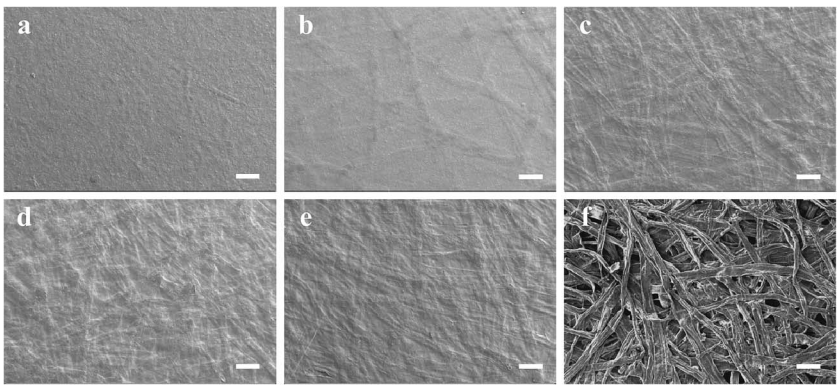

Fig. 5 Top-view SEM images of the transparent papers produced by TEMPO-oxidized wood fibers and/or NFC with an NFC content of (a) 100%, (b) 80%, (c) 50%, (d) 20%, and (e) 0%, and of (f) the regular paper. The scale bar is 100 μm.

Published on 26 August 2014. Downloaded by Northeastern University on 30/12/2015 02:25:48.

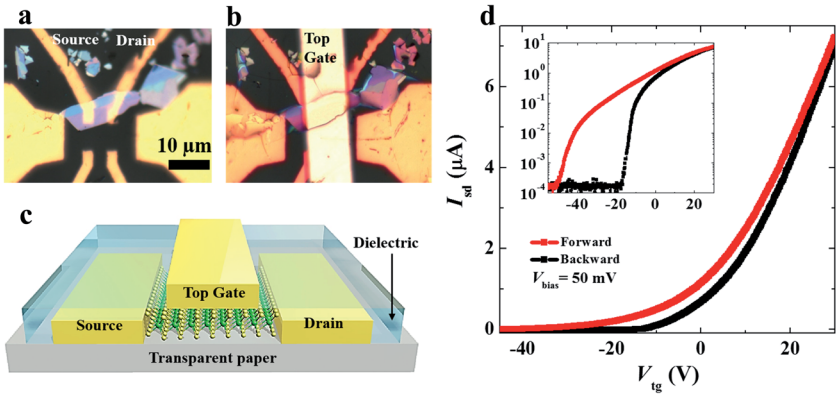

Fig. 6 (a) Optical image of a 20 nm thick MoS_2 device on transparent paper; (b) after 200 nm Al_2O_3 deposition, a 30 nm thick top gate electrode is patterned; (c) a schematic view of the MoS_2 field effect transistor shown in b; (d) transfer characteristic I_{sd}–V_{tg} with 50 mV applied bias voltage for the 20 nm thick MoS_2 FET at room temperature. The red and black curves indicate the forward and backward V_{tg} sweeping. Inset: the same I_{sd}–V_{tg} curve with I_{sd} in log scale.

various transparent paper substrates, and the data are demonstrated in Table 1. As the content of NFC within the transparent papers increases, L^* shows a slightly declining trend and no significant variations to the values of a^* and b^* are observed between the transparent papers. In comparison to the transparent paper without the NFC, $|\Delta a|$ and $|\Delta b|$ for the transparent papers with different NFC contents are less than 0.1 and 1.0, respectively. $|\Delta L|$ of the transparent paper with a NFC content of 20%, 50%, and 80% is less than 1.0. For the pure NFC film, $|\Delta L|$ is 2.37, showing a decrease of only 3.0%. Such tiny declines in L^*, a^*, and b^* among the various transparent papers are undetectable by the human eye; thus the approach to fabricate transparent papers with tunable light scattering effects will not lead to a severe color deviation.

Transparent paper provides excellent optical transmittance while simultaneously offering tunable light scattering behavior, which exhibits great potential for the fabrication of lighter, cheaper, and more flexible next generation "green" electronics. We recently laminated transparent paper with a high optical haze to the surface of an organic solar cell and the paper laminated solar cell presented a ~10% enhancement in power conversion efficiency (PCE).[21] Moreover, Ha *et al.* demonstrated a paper-based photovoltaic device by directly attaching a piece of paper with both high transparency and optical haze to the surface of a GaAs solar cell, showing a significant enhancement in PCE (23.91%) and a reduced angular dependence of reflectivity due to the combination of the index contrast and surface texture.[30] The transparent paper with the lowest diffuse light scattering (nanopaper) exhibits high transparency and superior surface smoothness, and thus is an ideal substrate for directly fabricating flexible electronics.[1,4,6,31] In this study, we fabricated a field effect transistor (FET) on a nanopaper. A 20 nm thick MoS_2 flake is first mechanically exfoliated by the classical scotch-tape technique onto the surface of the paper, followed by the patterning of 50 nm Au contact electrodes using a shadow mask method.[32] 200 nm Al_2O_3 is then directly deposited onto the MoS_2 flake through an aligned shadow mask in an electron-beam evaporator. Finally, a 30 nm Au top gate electrode is defined above the MoS_2 flake, as shown in Fig. 6a–c. Fig 6d displays an n-type unipolar behavior of the paper-supported 20 nm-thick MoS_2 FET, indicated by a source drain current, I_{sd}, (V_{sd} = 50 mV) as a function of the applied top gate voltage, V_{tg}. The I_{sd} (V_{tg}) curve shows a turning on at positive V_{tg} values (accumulation of electrons), while staying off at a negative V_{tg} window, which agrees with previously reported MoS_2 FETs on other substrates.[33–35] A large current on/off ratio $I_{on}/I_{off} \sim 1 \times 10^5$ is also achieved within the range of the applied V_{tg}. This demonstrates that our transparent paper is a promising and revolutionary substrate for next generation "green" electronics that fulfils the sustainable development of human society. Note that the transparent paper substrates are made of intrinsically green and renewable materials derived from wood. Current processes and materials used for the development of transparent papers are not all green, such as the use of TEMPO, and there is much development in the paper industry to replace these non-renewable parts. Examples include enzymatic treatment to replace TEMPO.[36,37] In the near future, green processes combined with wood-derived biomaterials will lead to fully renewable substrates as a robust replacement of plastics for a range of green electronics.

Table 1 CIELAB of the various transparent papers

	L^*	a^*	b^*
0%	79.17	−0.12	9.65
20%	78.56	−0.03	10.43
50%	78.53	−0.16	9.87
80%	78.15	−0.15	9.96
100%	76.80	−0.03	10.58

Conclusion

In summary, this study introduces a facile method to fabricate highly optical transparent paper with a tunable transmission haze by rationally regulating the weight ratio of TEMPO-oxidized

 This journal is © The Royal Society of Chemistry 2014

Published on 26 August 2014. Downloaded by Northeastern University on 30/12/2015 02:25:48.

wood fibers to NFC. The fabricated transparent paper not only exhibits a high transmittance of over 90% due to a high packing density, but also a varying light scattering effect tuned by managing the amount of the NFC in the paper. The scattering angular distribution of the various transparent papers ranges from 36° to 12°. Moreover, a MoS_2 field effect transistor was fabricated on the transparent paper of pure NFC, showing a large current on/off ratio, $I_{on}/I_{off} \sim 1 \times 10^5$. This earth-abundant, biodegradable and scalable transparent paper with a tailored transmission haze demonstrates the huge potential to expand the application of transparent paper on solar cells, outdoor displays, OLED light systems, and other devices.

Acknowledgements

Liangbing Hu would like to thank the Air Force Office of Scientific Research (AFOSR) Investigator Program for their funding. Zhiqiang Fang would like to thank the China Scholarship Council (CSC) for their financial support. We acknowledge the support of the Maryland NanoCenter and its NispLab. We would also like to thank Jeremy Munday and Joseph Murray for their help with the optical setup.

References

1 Y. Fujisaki, H. Koga, Y. Nakajima, M. Nakata, H. Tsuji, T. Yamamoto, T. Kurita, M. Nogi and N. Shimidzu, *Adv. Funct. Mater.*, 2014, **24**, 1657–1663.
2 M.-C. Hsieh, C. Kim, M. Nogi and K. Suganuma, *Nanoscale*, 2013, **5**, 9289–9295.
3 L. B. Hu, G. Y. Zheng, J. Yao, N. A. Liu, B. Weil, M. Eskilsson, E. Karabulut, Z. C. Ruan, S. H. Fan, J. T. Bloking, M. D. McGehee, L. Wagberg and Y. Cui, *Energy Environ. Sci.*, 2013, **6**, 513–518.
4 J. Huang, H. Zhu, Y. Chen, C. Preston, K. Rohrbach, J. Cumings and L. Hu, *ACS Nano*, 2013, **7**, 2106–2113.
5 M. Nogi, N. Komoda, K. Otsuka and K. Suganuma, *Nanoscale*, 2013, **5**, 4395–4399.
6 H. Zhu, Z. Xiao, D. Liu, Y. Li, N. J. Weadock, Z. Fang, J. Huang and L. Hu, *Energy Environ. Sci.*, 2013, **6**, 2105–2111.
7 M. Nogi and H. Yano, *Adv. Mater.*, 2008, **20**, 1849–1852.
8 A. N. Nakagaito, M. Nogi and H. Yano, *MRS Bull.*, 2010, **35**, 214–218.
9 T. T. Nge, M. Nogi and K. Suganuma, *J. Mater. Chem. C*, 2013, **1**, 5235–5243.
10 K. L. Chopra, P. D. Paulson and V. Dutta, *Prog. Photovoltaics*, 2004, **12**, 69–92.
11 A. V. Shah, H. Schade, M. Vanecek, J. Meier, E. Vallat-Sauvain, N. Wyrsch, U. Kroll, C. Droz and J. Bailat, *Prog. Photovoltaics*, 2004, **12**, 113–142.
12 A. Hongsingthong, T. Krajangsang, I. A. Yunaz, S. Miyajima and M. Konagai, *Appl. Phys. Express*, 2010, **3**, 051102–051103.
13 M. Zeman, O. Isabella, K. Jäger, R. Santbergen, S. Solntsev, M. Topic and J. Krc, *Energy Procedia*, 2012, **15**, 189–199.
14 S. Song, Y. Sun, Y. Lin and B. You, *Appl. Surf. Sci.*, 2013, **273**, 652–660.
15 T.-C. Huang, J.-R. Ciou, P.-H. Huang, K.-H. Hsieh and S.-Y. Yang, *Opt. Express*, 2008, **16**, 440–447.
16 H. P. Kuo, M. Y. Chuang and C. C. Lin, *Powder Technol.*, 2009, **192**, 116–121.
17 H. Meier, *Pure Appl. Chem.*, 1962, **5**, 37–52.
18 G. Chinga-Carrasco, *Nanoscale Res. Lett.*, 2011, **6**, 1–7.
19 N. Lavoine, I. Desloges, A. Dufresne and J. Bras, *Carbohydr. Polym.*, 2012, **90**, 735–764.
20 H. Zhu, S. Parvinian, C. Preston, O. Vaaland, Z. Ruan and L. Hu, *Nanoscale*, 2013, **5**, 3787–3792.
21 Z. Fang, H. Zhu, Y. Yuan, D. Ha, S. Zhu, C. Preston, Q. Chen, Y. Li, X. Han, S. Lee, G. Chen, T. Li, J. Munday, J. Huang and L. Hu, *Nano Lett.*, 2013, **14**, 765–773.
22 T. Saito and A. Isogai, *Biomacromolecules*, 2004, **5**, 1983–1989.
23 T. Saito, Y. Okita, T. T. Nge, J. Sugiyama and A. Isogai, *Carbohydr. Polym.*, 2006, **65**, 435–440.
24 C. Preston, Y. Xu, X. Han, J. N. Munday and L. Hu, *Nano Res.*, 2013, 1–8.
25 C. Preston, Z. Fang, J. Murray, H. Zhu, J. Dai, J. N. Munday and L. Hu, *J. Mater. Chem. C*, 2014, **2**, 1248–1254.
26 P. F. Smith, I. Chun, G. Liu, D. Dimitrievich, J. Rasburn and G. J. Vancso, *Polym. Eng. Sci.*, 1996, **36**, 2129–2134.
27 G. Kang, H. Park, D. Shin, S. Baek, M. Choi, D.-H. Yu, K. Kim and W. J. Padilla, *Adv. Mater.*, 2013, **25**, 2617–2623.
28 B.-T. Liu, Y.-T. Teng, R.-H. Lee, W.-C. Liaw and C.-H. Hsieh, *Colloids Surf., A*, 2011, **389**, 138–143.
29 M. Nogi and H. Yano, *Appl. Phys. Lett.*, 2009, **94**, 233117.
30 D. Ha, Z. Fang, L. Hu and J. N. Munday, *Adv. Energy Mater.*, 2014, **4**, DOI: 10.1002/aenm.201301804.
31 S. Purandare, E. F. Gomez and A. J. Steckl, *Nanotechnology*, 2014, **25**, 094012.
32 W. Bao, G. Liu, Z. Zhao, H. Zhang, D. Yan, A. Deshpande, B. LeRoy and C. N. Lau, *Nano Res.*, 2010, **3**, 98–102.
33 W. Bao, X. Cai, D. Kim, K. Sridhara and M. S. Fuhrer, *Appl. Phys. Lett.*, 2013, **102**, 042104.
34 S. Kim, A. Konar, W.-S. Hwang, J. H. Lee, J. Lee, J. Yang, C. Jung, H. Kim, J.-B. Yoo and J.-Y. Choi, *Nat. Commun.*, 2012, **3**, 1011.
35 B. Radisavljevic, A. Radenovic, J. Brivio, V. Giacometti and A. Kis, *Nat. Nanotechnol.*, 2011, **6**, 147–150.
36 M. Pääkkö, M. Ankerfors, H. Kosonen, A. Nykänen, S. Ahola, M. Österberg, J. Ruokolainen, J. Laine, P. T. Larsson, O. Ikkala and T. Lindström, *Biomacromolecules*, 2007, **8**, 1934–1941.
37 M. Henriksson, G. Henriksson, L. A. Berglund and T. Lindström, *Eur. Polym. J.*, 2007, **43**, 3434–3441.